

CONCEPTUAL DESIGN OF A DRIFT TUBE LINAC FOR PROTON THERAPY *

P.F. Ma, Q.Z. Xing[†], X.D. Yu, R. Tang, S.X. Zheng, X.L. Guan, X.W. Wang, Key Laboratory of Particle & Radiation Imaging (Tsinghua University), Ministry of Education, Beijing 100084, China also at Laboratory for Advanced Radiation Sources and Application, Tsinghua University, Beijing 100084, China

also at Department of Engineering Physics, Tsinghua University, Beijing 100084, China

C.P. Wang, J. Qiao, X.C. Xie, F. Yang, Y.H. Pu, Shanghai ATRACTRON Particle Equipment Company Limited, Shanghai 201800, China

Abstract

The conceptual design of an Alvarez-type Drift Tube Linac (DTL) for a proton therapy facility is described in this paper. The DTL will accelerate 16 mA proton beams from 3 MeV to 7 MeV. The main feature of the design is its low total RF peak power, which is only 201 kW. The error study of the Drift Tube Linac is also given in this paper.

INTRODUCTION

Proton therapy is blooming around the world in recent years according to the Particle Therapy Co-Operative Group (PTCOG) [1]. Under the support of the National Key Research and Development Program of China, a 7 MeV linac injector is designed for a synchrotron-based proton therapy facility. The linac mainly consists of an ECR source, a Low Energy Beam Transport line (LEBT), a 3 MeV Radio Frequency Quadrupole (RFQ) and a 7 MeV Drift Tube Linac (DTL).

PARAMETERS OF DTL

The DTL will accelerate 16 mA proton beams from 3 MeV to 7 MeV. The permanent magnet quadrupoles (PMQ) are used to focus the beam in the DTL. The PMQs are mounted in the drift tubes with an FD lattice. Compared with the electromagnetic quadrupoles, the PMQs do not need coils and water cooling. The PMQs have a simple structure which can effectively reduce the size of the drift tube and improve the acceleration efficiency.

The design of the DTL cavity aims at low total RF peak power. The cost can be saved if only one amplifier is used for the RFQ and the DTL. The tetrode-based RF power amplifier has been tested successfully to produce the peak power up to 500 kW at 325 MHz with the pulse width of 150 μ s and repetition rate of 1 Hz [2]. 500 kW can be regarded as the maximum peak power for the RFQ and the DTL from one amplifier. The parameters of the DTL cells have been optimized with respect to high effective shunt impedance per unit length Z_{T} to achieve a low peak power. The constant accelerating field per cell is adopted, and the average accelerating field E_0 is also optimized to reduce both length and power loss. The total

peak power of the RFQ is 177 kW according to the design result [3]. The peak power, including the beam power and 25% margin for the cavity power, is 201 kW, which is low enough for the amplifier.

The total length of the DTL is 3.41 m. The diameter of the cavity is 61.87 cm while the diameter of the drift tube is 8.4 cm and the bore radius is 0.7 cm [3]. The model of the DTL is presented in Fig. 1.

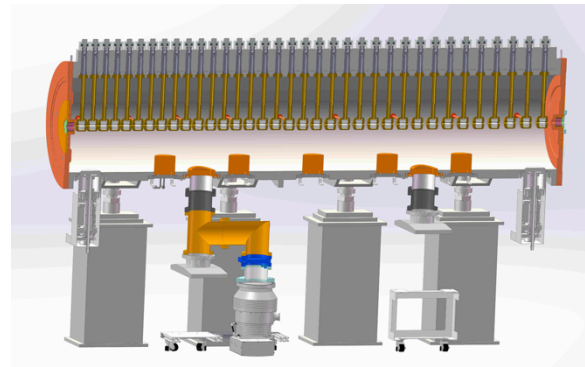


Figure 1: Model of the DTL cut along the beam axis.

The design parameters of the DTL are listed in Table 1.

Table 1: DTL Parameters

Parameter	Value
Ion type	Proton
Input beam energy	3 MeV
Output beam energy	7 MeV
Peak current	16 mA
RF frequency	325 MHz
Pulse length	40~100 μ s
Pulse repetition rate	0.5~10 Hz
Cell number	36
Average accelerating field	1.6 MV/m
Maximum surface field	0.55 Kilp
Total RF peak power for the DTL (25% margin)	201 kW
Total length	3.41 m

BEAM DYNAMICS

By optimizing the focusing strength at the exit of the RFQ, the DTL can be directly matched to the RFQ with-

04 Hadron Accelerators

A08 Linear Accelerators

* Work supported by the National Key Research and Development Program of China (grant number 2016YFC0105408).

[†] email address xqz@tsinghua.edu.cn

out a MEBT. Besides, the PMQs with the same gradient are adopted in the DTL [3].

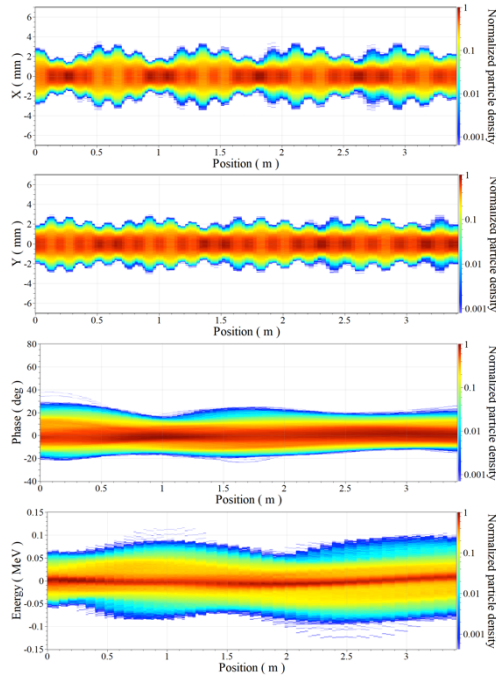


Figure 2: Beam dynamics in the DTL.

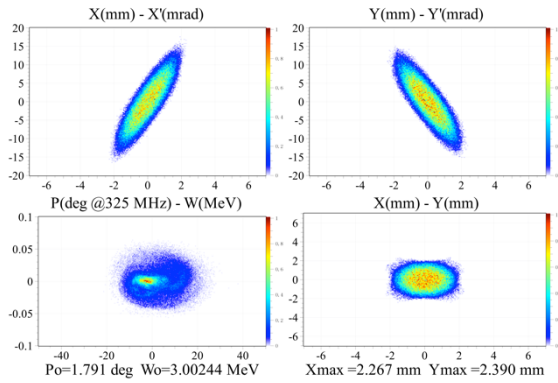


Figure 3: Phase space at the entrance of the DTL.

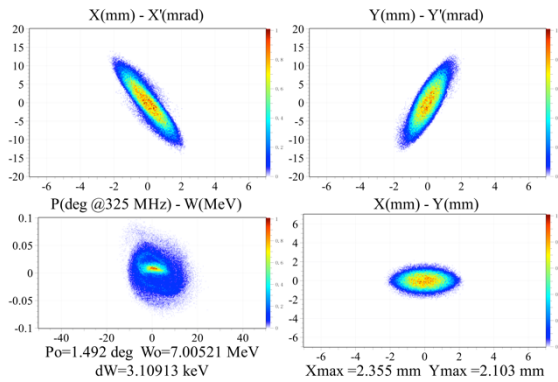


Figure 4: Phase space at the exit of the DTL.

The beam simulation is performed by the TRACEWIN code [4]. The simulated particle distribution from the RFQ exit is used as the input distribution at the entrance of the DTL. The beam dynamics of the DTL is shown in Fig. 2. The transmission rate of the DTL given by

TRACEWIN is 100%. The phase spaces at the entrance and exit of the DTL are given in Fig. 3 and Fig. 4. The growth of the normalized RMS transverse emittance is only 6% along the DTL.

ERROR ANALYSIS

Error analysis is important to test the robustness of the accelerator. The process of error analysis is as follows. First, the error sensitivities of individual errors are given by the beam simulation code. Then the tolerances of individual errors are defined by error sensitivities and practical abilities. At last, the simulations considering all the errors are carried out within the defined tolerances, to check whether the output beam meets the requirements of the accelerator.

Error Analysis Strategy

As the bore radius is much larger than the beam radius (see Fig. 2), the particles are not easy to lose if the individual errors are small. The beam loss is not a good criterion to judge error sensitivities.

Emittance growth is a good standard to characterize error sensitivities if beam loss is not serious. The emittance grows naturally along the linac. The additional emittance growth due to the errors can be defined as [5]:

$$\Delta \varepsilon_k = \frac{\varepsilon_{out,ERR,k} - \varepsilon_{out,NO,k}}{\varepsilon_{out,NO,k}} \quad (1)$$

where $\varepsilon_{out,ERR,k}$ is the output emittance with individual or combined errors in the k -plane, $\varepsilon_{out,NO,k}$ is the output emittance without errors in the k -plane.

Individual Errors

Individual errors consist of 1) input beam errors: position and divergence of the beam center, emittance change of the beam, phase and energy jitter, mismatch of the Twiss parameters, current jitter; 2) quadrupole errors: transverse displacement, rotation and gradient and 3) RF field errors: field amplitude and phase, field and phase of the klystron.

Due to limited space, only some results of the individual errors are discussed. Some individual errors have little effect on the transverse emittance while the others have a small impact on the longitudinal emittance.

The position and divergence error of the beam center will lead to the beam loss and transverse additional emittance growth (see Fig. 5). The values of the error in x -plane and y -plane are the same for each point. When the beam loss is severe, the beam size is getting smaller. Therefore, the transverse additional emittance growth is minus, but it does not mean that the beam quality is better.

If the mismatch of the Twiss parameters is large enough that some input particles are out of the acceptance phase space of the DTL, the beam loss occurs. The transverse additional emittance growth is the joint action of mismatch and beam loss (see Fig. 6). The values of α are opposite numbers in x -plane and y -plane. The values of α in Figure 6 represent the value in x -plane.

Content from this work may be used under the terms of the CC BY 3.0 licence (© 2018). Any distribution of this work must maintain attribution to the author(s), title of the work, publisher, and DOI.

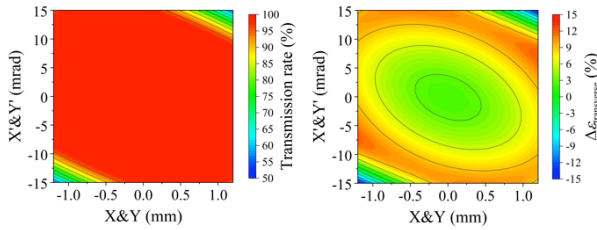


Figure 5: Error sensitivity due to the position and divergence error (left: transmission rate; right: transverse additional emittance growth).

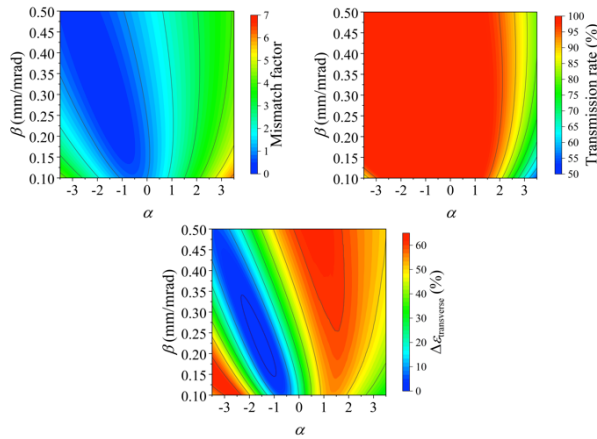


Figure 6: Error sensitivity due to the mismatch of the Twiss parameters error (top left: mismatch factor; top right: transmission rate; bottom: transverse additional emittance growth).

Many other discussions on the individual errors are not given in this paper. The error sensitivities are studied and the main error tolerances of the DTL are listed in Table 2 [3].

Table 2: The Main Error Tolerances of the DTL

Input beam tolerances		Quadrupole tolerances	
Position	± 0.3 mm	Displacement	± 0.17 mm
Divergence	± 5.5 mrad	Gradient	$\pm 3\%$
Mismatch	15%	amplitude	
Energy jitter	± 0.02 MeV	Rotation	$\pm 3^\circ$
Phase jitter	$\pm 4^\circ$	(x, y axis)	
Field tolerances		Rotation	$\pm 0.6^\circ$
Amplitude	$\pm 2\%$	(z axis)	
Phase	$\pm 2^\circ$		

Combined Errors

After the error tolerances are given, the comprehensive error study of the beam transmission rate is performed with combinations of all the individual errors listed above, including the input beam errors, the quadrupole errors and the RF field errors. The simulation is performed for 5000 times and 100000 macro-particles in each run. The errors are uniformly random distributed within the tolerances. The simulation results are shown in Fig. 7. Beam transmission rate is larger than 99% with the probability of

99%. The transverse additional emittance growth is smaller than 21% with the probability of 95%.

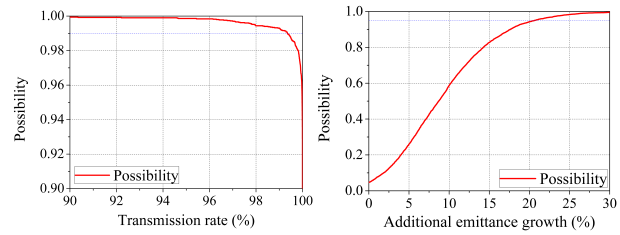


Figure 7: Possibility of the transmission rate (left) and the transverse additional emittance growth (right) of the DTL.

RF DESIGN RESULT

The DTL cavity is modelled by SUPERFISH code [6] with stems, post couplers and tuners. The RF frequency calculated by the code is 325 MHz. The accelerating field distribution along the beam axis of the cavity is given in Fig. 8.

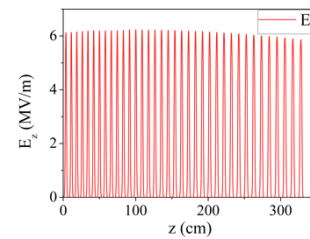


Figure 8: Accelerating field distribution along the beam axis of the DTL cavity.

CONCLUSION AND FUTURE WORK

The design of the DTL for proton therapy has been presented. The main feature of the DTL is its low RF power cost. The error analysis shows the DTL can perform well under the defined error tolerances.

The engineering design of the DTL is under-discussed. The construction of the DTL is scheduled to be finished by the end of 2019. The beam test of the DTL is expected by September 2020.

ACKNOWLEDGEMENT

Special thanks to B.C. Wang for his great help. We acknowledge the support of the National Key Research and Development Program of China (grant number 2016YFC0105408).

REFERENCES

- [1] PTCOG, <http://www.ptcog.ch>
- [2] Y. Lei *et al.*, “High-power RF test of coaxial couplers for the injection linac of XiPAF”, presented at IPAC’18, Vancouver, Canada, May 2018.
- [3] P.F. Ma *et al.*, “Physical design of the proton linac injector for the synchrotron-based proton therapy system in China”, submitted for publication.
- [4] *Tracewin documentation*, D. Uriot, N. Pichoff, CEA Saclay, July 2017.

- [5] R. De Prisco *et al.*, “Error study on the normal conducting ESS linac”, in *Proc. LINAC’14*, Geneva, Switzerland, Sep. 2014, paper THPP042, pp. 942-944.
- [6] J.H. Bilen, L.M. Young, “Poisson Superfish”, LA-UR-96-1834, Rev, 2005.